

Retrofitting of Beam-Column Joint Using CFRP and Steel Plate

N. H. Hamid, N. D. Hadi, K. D. Ghani

Abstract—This paper presents the retrofitting of beam-column joint using CFRP (Carbon Fiber Reinforced Polymer) and steel plate. This specimen was tested until failure up to 1.0% drift. This joint suffered severe damages and diagonal cracks at upper crack at upper column before retrofitted. CFRP were wrapped at corbel, bottom and top of the column. Steel plates with bonding were attached to the two beams and the jointing system. This retrofitted specimen is tested again under lateral cyclic loading up to 1.75% drift. Visual observations show that the cracks started at joint when 0.5% drift applied at top of column. Damage of retrofitted beam-column joint occurred inside the CFRP and it cannot be seen from outside. Analysis of elastic stiffness, lateral strength, ductility, hysteresis loops and equivalent viscous damping shows that these values are higher than before retrofitting. Therefore, it is recommended to use this type of retrofitting method for beam-column joint with corbel which suffers severe damage after the earthquake.

Keywords—Beam-Column joint, ductility, stiffness, retrofitting.

I. INTRODUCTION

EARTHQUAKE can cause reinforced concrete buildings to collapse, loss of lives and also staggering economic losses. Most of the structures in Malaysia are not able to resist moderate or major earthquake loading. Under seismic loading, it is important for RC building to have lateral resistance capacity against brittle failure. Non-seismic design buildings which designed using non-seismic code of practice are vulnerable to earthquake excitations. Since demolishing and reconstructing RC buildings are expensive, retrofitting the small fraction of structural components and building may offer a workable solution for ensuring the safety of the building and people.

Fiber Reinforced Polymer (FRP) is a popular material which normally used in strengthening RC structural elements in recent years. Experimental results of seismic resistance of FRP retrofitted column improved the lateral strength, stiffness and ductility significantly [1]. Failure of beam-column joint connections can easily lead to the catastrophic collapse of a frame building as often observed in recent earthquakes. Laboratory testing and analysis of the results show that non-seismic structures are vulnerable to earthquake loading.

Failure mechanism of beam-column joint when assessing the nominal strength of a member was predicted to be associated with material strain and stress relationship together with the levels achieved after earthquake [2].

Shear failure usually occur as a result of inadequate transverse reinforcement in the joint and weak-column/strong beam design [3]. Diagonal shear failure in column is the main cause of soft-storey mechanism in RC buildings. High rise buildings are highly exposed to frame damages because it tends to have soft-storey mechanism failure. Soft-storey mechanism is the most frequent failure mode of RC moment frame building [4]. This failure is due to insufficient of reinforcement bars in the beam-column joint and column. When a column is damaged, it forms a plastic hinge zone (PHZ) near the joint and upper part of the column. Therefore, the structure will be more vulnerable to earthquake attack and may experience partial collapse of the structure after the earthquake. Retrofitting of structures should be made to the damage buildings to increase their strength, stiffness and ductility after the earthquake attack.

There are many types of retrofitting method which available for fixing joints. Some of the famous ones include steel plate jacketing, plastic hinge relocation and textile reinforced mortar [5], [6]. An experimental work has been conducted on the steel plate rehabilitation of RC beam-column joint and the seismic retrofitting showed the excellence performance after retrofitting [7]. Many researchers opted to use carbon fiber as the external reinforcement material because of its high strength to weight ratio and good fatigue properties [8].

The intention of this study is to study the seismic retrofitting of beam-column joint with corbel tested under lateral cyclic loading using CFRP (Carbon Fiber Reinforced Polymer) and steel plate bonding. The experimental work was conducted and tested up to the maximum failure of the structures. The sub-assembly of exterior beam-column joint from precast two-storey school building was constructed in Heavy Structural Laboratory, Faculty of Civil Engineering, UiTM.

Fig. 1 shows selected sub-assembly of beam-column joint of a two-storey precast school building. The selected joint consists of one column with two tier corbels and two beams are seating on the corbel supported by the extruder bars which coming out from the corbel. The support conditions at both beams are pinned jointed where the beam is clamped using two steel plates and tight together using four high yield bolts and thread rods. The end condition of column-foundation is designated as partially fixed where the column is jointed to foundation using four extruder bars coming out from

N.H. Hamid is with Faculty of Civil Engineering, Universiti Teknologi Mara, 40450, Shah Alam, Selangor, Malaysia (phone: 006-0173159303, email: norha454@salam.uitm.edu.my).

N.D. Hadi is a PhD student at Universiti Teknologi Mara, 40450, Shah Alam, Selangor, Malaysia (phone: 006 -0129707358, email: diyana angelica@yahoo.com).

K.D. Ghani is a PhD Student at Universiti Teknologi Mara, 40450, Shah Alam, Selangor, Malaysia (phone: 006-0195708781, email: kaymageeston@yahoo.com).

foundation and the gaps of the rod are grouted using non-shrinkage grout.

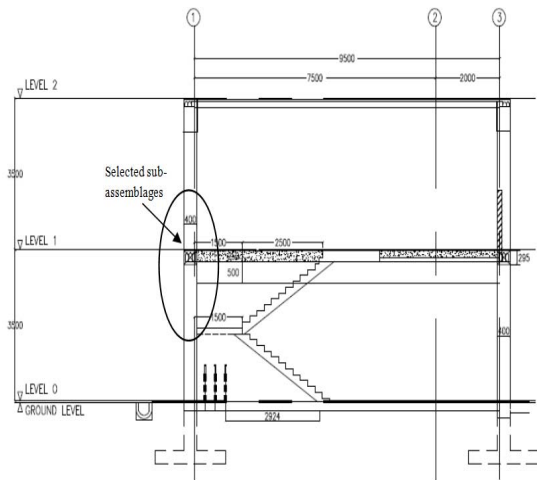


Fig. 1 Front view of two-storey prototype school building

Dimensions of the column and beam are 4000x400x400mm and 3500x750x500mm, respectively while dimension of the corbel is given by 1000x400x250mm. The whole sub-assemblage of exterior beam-column joint were constructed using concrete Grade 50 ($f_{cu}=50MPa$) and high steel bars with $f_y=460N/mm^2$. After construction completed, the specimen was labeled as BC-23E and tested under quasi-static lateral cyclic loading. The specimen was tested up to 1.0% drift where the beam-column joint experienced severe damage such as spalling of concrete, cracks and bending of longitudinal bars [9].

II. RETROFITTING AND STRENGTHENING OF BEAM-COLUMN JOINT

The retrofitting and strengthening of beam-column joint take place using CFRP and steel plate. The first step of retrofitting and strengthening the beam-column joint is to treat and close the gaps of cracks. This is to ensure that the cracks are properly treated prior to retesting of specimen under lateral cyclic loading. The diagonal crack at top column was treated with epoxy to cover up the structural cracks. The wrapping of CFRP sheets on prime coat epoxy resin takes place once the epoxy injection grouting dried. The top column is retrofitted with three layers of CFRP sheets while the bottom column and corbel were retrofitted with two layers of CFRP sheets. The transverse beam near the joint region was strengthened using 2500mm x 750mm x 8mm steel plate on both side of the joint.



Fig. 2 The specimen BC-23ER is ready for testing

After the crack was repaired, the steel plate was then bolted to both side of the joint region using 23 stainless steel M16 anchor. Before the plate is attached to the specimen, fifteen holes with size of 16mm were drilled on the beam surface. After that, the plates were bonded to the beam-column joint and bolted with the anchor bolts. Fig. 2 shows the specimen BC-23ER after retrofitted with CFRP and steel plate bonding which is ready for testing.

III. EXPERIMENTAL SET-UP AND INSTRUMENTATION

Nine (9) numbers of LVDT are used to measure the lateral displacement, movement of foundation beam and sliding of beam during lateral cyclic loading. Fig. 3 shows the location of LVDTs and double actuator which attached to top of the column.

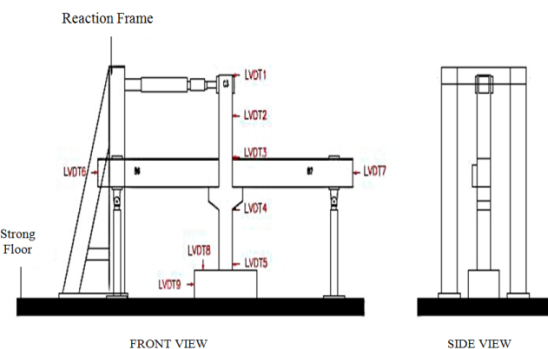


Fig. 3 Location of double actuator and LVDTs from front elevation of the specimen

Retrofitting of beam-column joint was retested again using control displacement method at $\pm 0.01\%$ drift until $\pm 1.75\%$ drift with an increment of 0.05% and 0.1%. The applied drift for the retrofitted specimen is similar to before retrofitting which is $\pm 0.01\%$, $\pm 0.05\%$, $\pm 0.1\%$, $\pm 0.2\%$, $\pm 0.3\%$, $\pm 0.4\%$, $\pm 0.5\%$, $\pm 0.6\%$, $\pm 0.75\%$, $\pm 0.8\%$, $\pm 1.0\%$, $\pm 1.25\%$, $\pm 1.5\%$ and $\pm 1.75\%$. Two cycles of loading were applied for each drift.

Fig. 4 shows the loading regime (displacement versus number of cycles) for the retrofitting beam-column joint. Table I shows the designation of beam-column joint. The beam-column joint before retrofitting is labeled as BC-23ER.

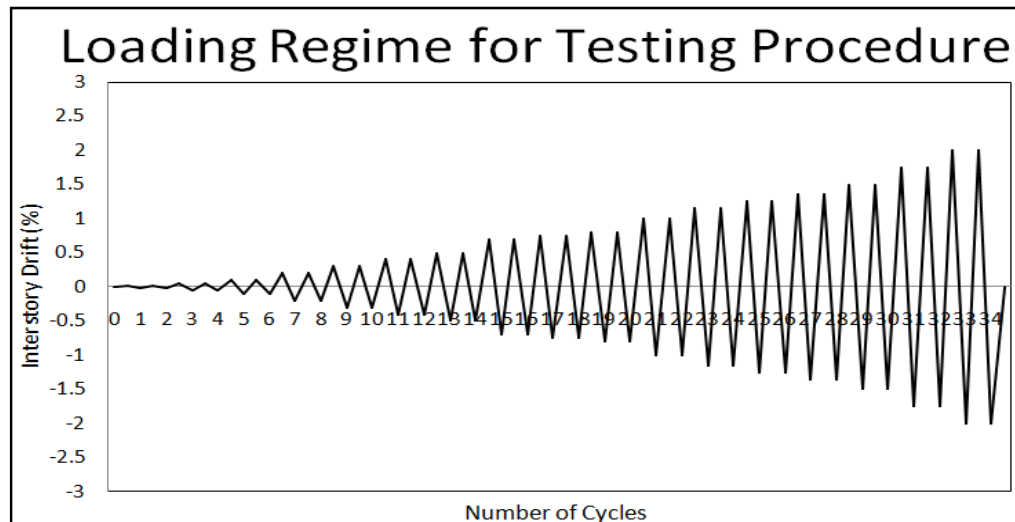


Fig. 4 Loading regime for testing the specimen

TABLE I
DESIGNATION OF BEAM-COLUMN JOINT

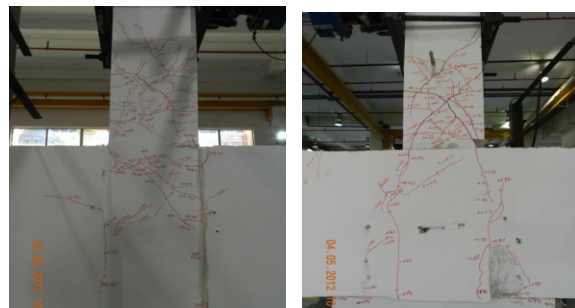
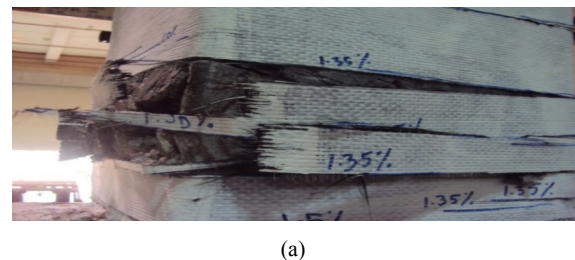
Specimen Designation	Test condition and retrofit schemes using CFRP and steel plate
BC-23E	Before retrofitting
BC-23ER	Repaired specimen BC23E after control test, then rehabilitated with three CFRP sheets and two 8mm steel plate.

IV. EXPERIMENTAL RESULTS AND DISCUSSION

A. Visual Observations

The first crack found on the control specimen occurred at $\pm 0.1\%$ drift at corbel-column interfaces under lateral cyclic loading. At $\pm 0.5\%$ drift, many hairline cracks were observed starting from top of column and beam-column joint. Diagonal cracks started to shown at cast-in-place area at beam-column joint as well as flexural cracks on beam at 0.5% drift. At $\pm 1.0\%$ drift, an extension of the diagonal crack with 5mm width formed which later result in diagonal shear crack. The diagonal shear crack was formed due to the strong beam-weak column design known as soft storey mechanism.

Fig. 5 shows the diagonal shear crack at top column after $\pm 1.0\%$ drift before retrofitting. During retesting, there are no visible hairline cracks or tearing of the CFRP sheet on the beam and column at 0.01% drift to 0.5% drift. The formation of crack can only be seen along the interface of the column to beam at 0.6% drift. At 1.5% , minor spalling of concrete started to shown at the corner of the side of the column. When the drift is increased up to 1.75% drift, the column failed and tears the CFRP layers showing the large crack and spalling of concrete under the layers to tear completely. At this point, the specimen experienced a complete disintegration at the top column. The test revealed that the reinforcement bar has bended which causes the failing of the top column as shown in Fig. 6.

Fig. 5 Diagonal shear crack at top column after $\pm 1.0\%$ drift before retrofitting; (a) front view and; (b) back view

(a)



(b)

Fig. 6 Damages on BC-23ER; (a) large tear and; (b) bended reinforcement after $\pm 1.75\%$ drift after retrofitting

B. Hysteresis Loop

Hysteresis loop is used to measure the behavior of structure starting from elastic range until non-elastic range. It can be obtained by plotting the graph of load vs. displacement from loading and unloading branch to complete one cycle of movement. From hysteresis loops, the parameter such as maximum lateral displacement, stiffness, ductility and equivalent viscous damping can be determined. The hysteresis loops of specimen before retrofitting is shown in Fig. 7 and hysteresis loops after retrofitting is shown in Fig. 8. From these graphs, specimen BC23ER has higher lateral strength and bigger ductility. Specimen BC23ER can sustain load up to $\pm 1.0\%$ drift with a significant increase in stiffness and ductility before undergo strength degradation from $\pm 1.25\%$ to 1.75% drift.

The seismic retrofitting behavior of the beam-column joint after retrofitting depends on the number of CFRP layers applied to the damage area. Since the specimen was retrofitted with CFRP and steel plate, the stiffness of the beam-column joint with corbel also increases and can withstand higher loading with smaller displacement as compared to the before retrofitted specimen as shown in Fig. 7.

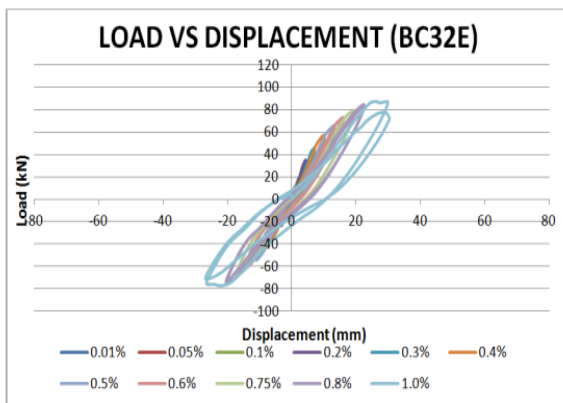


Fig. 7 Hysteresis loops for BC-23E

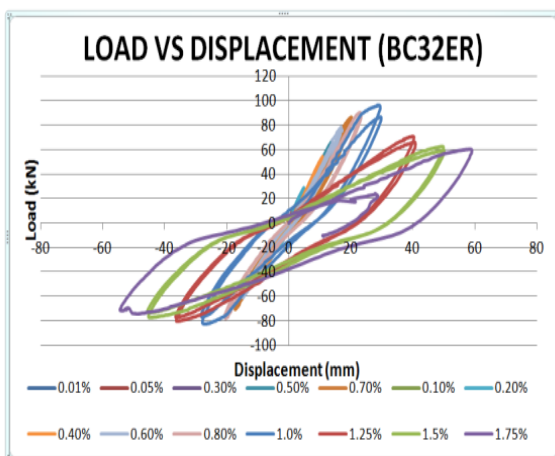


Fig. 8 Hysteresis loops for BC-23ER

C. Lateral Strength

The inelastic behavior of the control and retrofitted beam-column joint in terms of load-displacement (hysteresis loop) relationship was compared. Based on the result, both load carrying lateral strength capacities of specimen (BC-23E and BC-23ER) under linear elastic region and continue to reach the ultimate load under inelastic behavior before reaching strength degradation at $\pm 1\%$ drift for control specimen and 1.75% drift for retrofitted specimen.

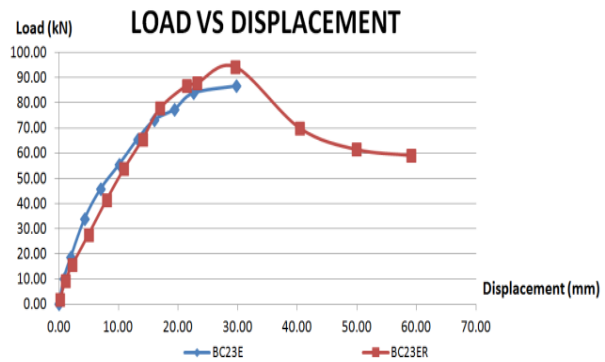


Fig. 9 Load vs. displacement for BC-23E and BC-23ER

Fig. 9 shows the load vs. displacement curve for BC-23E and BC-23ER. Both specimen undergo linear behavior starting from 0.01% to 0.6% , therefore the yield point for both specimen is observed at 0.6% drift. The yield strength had increased by more than 5% at the 0.6% drift. The before retrofitted specimen proceeds to an ultimate load of 86.79 kN at 1.0% drift while the ultimate load for retrofitted specimen is 94.2 kN . This proves that the lateral strength of the retrofitted specimen increased by 7.9% . The strength degradation that starts to occur after 1.0% drift for the retrofitted specimen is due to the diagonal shear failure formed at the top column.

D. Stiffness and Ductility

Stiffness is ratio of the force required to the specified deflection. Stiffness values in the positive and negative direction were determined by dividing the maximum load reached within a cycle by the corresponding displacement. Elastic stiffness (K_e), secant stiffness (K_{sec}) and effective stiffness (K_{eff}) are determined based on the load to the displacement data obtained during testing. K_e , K_{sec} and K_{eff} can be expressed using (1)-(3).

$$K_e = \frac{\text{Yield Load, } F_y}{\text{Yield Displacement, } \Delta_y} \quad (1)$$

$$K_{sec} = \frac{\text{Ultimate Load} - \text{Yield Load, } F_u - F_y}{\text{Ultimate Displacement} - \text{Yield Displacement, } \Delta_u - \Delta_y} \quad (2)$$

$$K_{eff} = \frac{\text{Ultimate Load, } F_u}{\text{Ultimate Displacement, } \Delta_u} \quad (3)$$

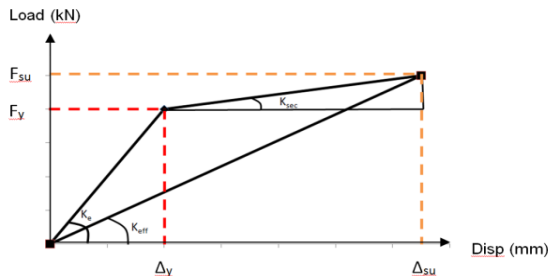


Fig. 10 Lateral displacement, stiffness and ductility of BC23E

The stiffness pattern for the first three drift values for specimen BC-23E and specimen BC-23ER are different. Generally, the stiffness value for both specimens should decrease as the target drift increases. However, the stiffness for control specimen increases from 0.01% to 0.05% and proceed to decrease until 1.0% drift. Even though both cycles experienced stiffness degradation, the stiffness for retrofitted specimen at yielding point increased by 46%. Tables II and III show the lateral displacement, lateral load, stiffness, and displacement ductility for specimens BC-23E and BC-23ER, respectively.

The ductility of the specimen is determined based on the ratio of lateral displacement (Δ_y). The acceptable ductility value for a reinforced concrete structure to withstand a mild earthquake is between 3 and 6. The displacement ductility for BC-23ER at failure (1.75% drift) has shown to be increase by 46% as compared BC-23E at failure (1.0% drift) for the first cycle. The significant increase in ductility is due to the CFRP layers provided together with steel plate. CFRP sheets have high tensile strength; therefore it helps to hold the column in place for a much longer time before tearing at high applied load. The displacement ductility factor for the control specimen was shown to be less than 3. This indicates that it cannot sustain mild earthquake. However, when the specimen was retrofitted using CFRP sheet and steel plate, the displacement ductility factor increased to an ultimate of 3.49. This result proves that the lateral strength provided by CFRP managed to increase the ductility of the specimen.

TABLE II
STIFFNESS AND DUCTILITY OF BEAM-COLUMN JOINT FOR BC-23E

BC-23E					
Target Drift (%)	Lateral displacement (mm)	Lateral Load (kN)	Elastic Stiffness, Ke (kN/mm)	Secant Stiffness, Ksec (kN/mm)	Ductility
0.01	0.02	0.06	8.43	-	0.00
0.05	0.84	10.13	12.54	-	0.05
0.10	2.0	18.68	7.37	-	0.13
0.20	4.32	33.93	6.57	-	0.27
0.30	7.00	45.81	4.43	-	0.44
0.40	10.10	55.51	3.13	-	0.63
0.50	13.18	65.57	3.27	-	0.82
0.60	15.98	73.23	2.73	-	1.00
0.75	19.36	77.45	-	1.25	1.21
0.80	22.55	83.90	-	1.63	1.41
1.00	29.77	86.79	-	0.40	1.86

TABLE III
STIFFNESS AND DUCTILITY OF BEAM-COLUMN JOINT FOR BC-23ER

BC-23ER					
Target drift (%)	Lateral displacement (mm)	Lateral Load (kN)	Elastic stiffness, Ke (kN/mm)	Secant stiffness, Ksec (kN/mm)	Ductility
0.01	0.18	1.87	10.39	-	0.01
0.05	1.08	9.22	8.17	-	0.06
0.10	2.22	15.49	5.50	-	0.13
0.20	4.94	27.6	4.45	-	0.29
0.30	7.98	41.41	4.54	-	0.47
0.40	10.89	53.7	4.22	-	0.64
0.50	14.03	65.51	3.76	-	0.83
0.60	16.93	77.75	4.22	-	1.00
0.75	21.41	86.73	-	2.00	1.26
0.80	23.17	87.75	-	0.58	1.37
1.00	29.59	94.2	-	1.00	1.75
1.25	40.38	69.91	-	-2.25	2.39
1.50	49.88	61.42	-	-0.89	2.95
1.75	59.05	59.06	-	-0.32	3.49

E. Energy Dissipation

The hysteresis energy dissipation is measured by equivalent viscous damping theory for a system with hysteretic behavior [6]. Equivalent viscous damping (ξ_{eq}) is the value of damping which makes equal the displacement of the equivalent linear system and the target displacement. Equivalent viscous damping can be calculated by using (4).

$$\xi_{eq} = \frac{1}{4\pi} \times \frac{E_D}{E_{SO}} \times 100\% \quad (4)$$

where E_D is the area enclosed by the hysteresis loops and E_{SO} is the area under the equivalent linear hysteresis curve. Fig. 11 shows a single hysteresis loops with indication of energy dissipation, E_D and strain energy, E_{SO} . Large displacement in the hysteretic loop shows that BC-23ER absorbs more energy and strengthened the beam-column joint during earthquake loading.

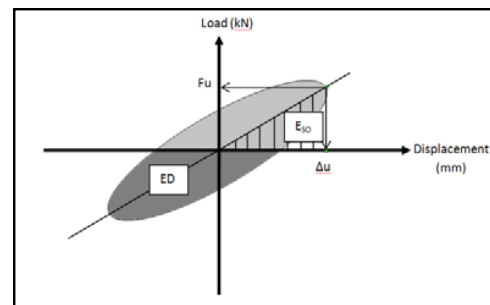


Fig. 11 Hysteresis loop with indication of ED and strain energy

Fig. 12 shows the comparison of equivalent viscous damping during the first cycle of specimen BC-23E and BC-23ER. The initial equivalent viscous damping for specimen BC-23E has higher values compared to specimen BC-23ER which due to the fact that elastic stiffness has reduced for specimen BC-23ER. However, the equivalent viscous

damping for specimen BC-23ER is higher than original specimen because CFRP and steel plate give better confinement concrete and prevent the column to fail earlier than specimen BC-23E.

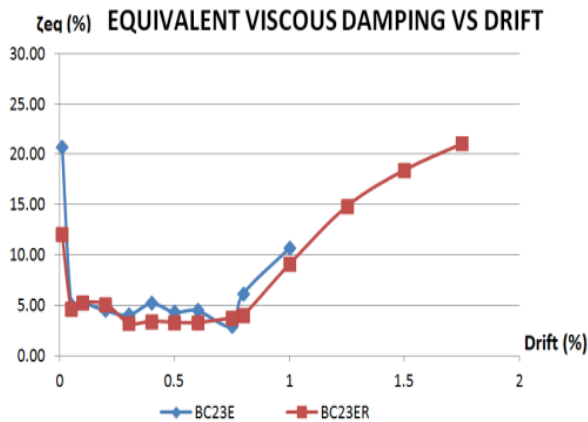


Fig. 12 Comparison of equivalent viscous damping for first cycle of specimen BC-23E and BC-23ER

V. CONCLUSION

Based on the visual observation, results and data interpretation, the following conclusion can be drawn as follows:

- 1) The overall performance of the retrofitted beam-column joint had increased when compared to the control specimen. This indicates that the retrofitting method was able to strengthen the beam-column joint with corbel under lateral cyclic loading.
- 2) The control specimen experienced diagonal shear failure at the top column that contributed to the soft-storey mechanism phenomenon when tested under lateral cyclic loading at 1% drift. However, the retrofitted specimen experienced cracking at interfaces and rupture of CFRP sheet and banded reinforcement when retested under lateral cyclic loading at 1.75% drift.
- 3) By retrofitting the exterior beam-column joint with CFRP, the lateral strength is increased by 5% for the beam-column joint. The stiffness of beam-column joint also increases after retrofitting. At yield point, the stiffness increased by nearly 46% for the first cycle and 29% for the second cycle in the positive direction. The ductility of the retrofitted beam-column joint has increased to almost twice the value of the control specimen after retrofitting as compared to before retrofitting in the first cycle while the equivalent viscous damping for the retrofitted specimen is higher than the control specimen.

ACKNOWLEDGMENT

This research was sponsored by FRGS (Fundamental Research Grants Scheme, MOHE (Ministry of Higher Education), Putrajaya, Malaysia and managed by RMI

(Research Management Institute), University Teknologi MARA, Malaysia. Special thanks and gratitude to the all technicians at Heavy Structural Laboratory, UiTM for their assistance and support for making the research project successful.

REFERENCES

- [1] Ozcan O., Binici B., and Ozcebe G. (2008), Improving seismic performance of deficient reinforced concrete columns using carbon fiber-reinforced polymers. *Journal of Engineering Structures*, 30 (1), p.1632-1646.
- [2] Akguzel U. and Pampanin S. (2012) Assessment and Design Procedure for the Seismic Retrofit of Reinforced Concrete Beam-Column Joints using FRP Composite Materials. *Journal of Composites for Construction*, 16 (1), p.21-34.
- [3] Ghobarah, A. and Said, A. (2002) Shear-strengthening of beam-column joint. *Journal of Engineering Structures*, 24 (1), p.881-888.
- [4] Plumier, A. Doneux, C. Stoychev, L. and Demarco, T. (2005) Mitigation of soft storey failures of R.C. structures under earthquake by encased steel profiles. *Proceedings of the Fourth International Conference on Advances in Steel Structures 13-15 June 2005, Shanghai, China*, 2 (1), p.1193-1198.
- [5] Sasmal S., Ramanjaneyulu K, Novák B., Srinivas V, Kumar K. S., Korkowski C, Roehm C., Lakshmanan N. and Iyer N. R. (2011) Seismic retrofitting of nonductile beam-column sub assemblage using FRP wrapping and steel plate jacketing. *Journal of Construction and Building Materials*, 25 (1), p.175-182.
- [6] Dalalbashi, A. Eslami, A. and Ronagh, H.R. (2012) Plastic hinge relocation in RC joints as an alternative method of retrofitting using FRP. *Journal of Composite Structures*, 94 (1), p.2433-2439.
- [7] Yen, J. and Chien, H. (2010) Steel plates rehabilitated RC beam-column joints subjected to vertical cyclic loads. *Journal of Construction and Building Materials*, 24 (1), p.332-339.
- [8] Belouar, A., Laraba, A., Benzaid, R. and Chikh, N. Abstract of papers, *The 2nd International Conference on Rehabilitation and Maintenance in Civil Engineering (ICRMCE-2)*, Solo, Indonesia; Sebelas Maret University: Solo, Indonesia, 2012; B6-018.
- [9] Kay, A.G. and Hamid, N.H. (2012), Seismic Performance of SFRC Beam-Column Joint with Corbel Under Reversible Lateral Cyclic Loading, *IACSIT International Journal of Engineering and Technology*, ISSN 1793-8236, Vol.4, No.1, February 2012, p.76-80.